Available online at www.sciencedirect.com
ScienceDirect
Catalysis Today 125 (2007) 40–47
CATALYSIS TODAY
www.elsevier.com/locate/cattod

Kinetics of hydrogen peroxide synthesis by direct combination of H_2 and O_2 in a microreactor

Yury Voloshin *, Raghunath Halder, Adeniyi Lawal

New Jersey Center for Microchemical Systems, Department of Chemical, Biomedical, and Materials Engineering, Stevens Institute of Technology, 1 Castle Point, Hoboken, NJ 07030, USA

Available online 2 March 2007

Abstract

Hydrogen peroxide is an industrially important oxidant with a growing number of applications in the chemical and textile industries, and in environmental remediation. Production of H_2O_2 by the direct combination of H_2 and O_2 is much less energy-intensive than the currently used anthraquinone autoxidation method, but it has not been implemented commercially because of the explosive nature of H_2 and O_2 mixtures. In this work, hydrogen peroxide was safely produced by direct combination of hydrogen and oxygen in a microreactor in the explosive regime. Concentrations as high as 1.3 wt% H_2O_2 were achieved. Optimum ranges of the temperature and pressure for H_2O_2 production were determined, and the reaction was shown to be free of mass transfer limitations at the conditions of kinetic experiments. A plan for obtaining the overall kinetics of direct H_2O_2 formation is described, which involves the determination of rate expressions of H_2O_2 synthesis, and of consequent decomposition of H_2O_2. A mechanism for the H_2O_2 synthesis reaction is proposed on the basis of past research and kinetic data. A rate expression is derived based on the proposed mechanism, and kinetic data were used to calculate the kinetic constants. This is the first step toward the determination of complete kinetics of direct H_2O_2 formation.

Keywords: Hydrogen peroxide; Direct synthesis; Microreactor; Palladium catalyst

1. Introduction

1.1. Overview

Hydrogen peroxide is an industrially important chemical with a large number of applications. It is widely used as an environmentally friendly oxidant for soil remediation and in the paper and textile industries, where it replaces chlorine bleaches. Global demand for hydrogen peroxide has been growing for the last two decades due to rising environmental concerns [1]. Since the middle of the twentieth century, the large majority of commercial hydrogen peroxide was produced by the anthraquinone autoxidation (AO) method [1]. The AO process has several important drawbacks. Hydrogen peroxide must be produced in large amounts and at high concentrations of about 70% [2] in order for the process to be profitable, which requires an energy-intensive distillation step for increasing the H_2O_2 concentration. The high concentrations are required for minimizing the liquid volume that needs to be transported to the end-users, thus decreasing the transportation expenses. Since many end-users require concentrations as low as 0.5–10 wt% [3], dilution by the end-user adds an additional expense.

A direct combination (DC) of hydrogen and oxygen in the presence of a catalyst and a solvent seems to be the simplest method of producing hydrogen peroxide. The potential commercial importance of this process attracted a large number of inventors since the first DC patent of Henkel and Weber [4]. Even though a large number of patents were issued for different variations of this process over the years [5–14], the DC method has not reached the commercialization stage yet due to a number of technical challenges. First, hydrogen and oxygen form a flammable mixture over a wide range of concentrations (5–96% H_2 in O_2). Thus, in most patents the preferred operating gas composition is below the explosive limit, and at high pressures on the order of several thousand psi, which are required in order to increase the concentration of dissolved hydrogen in the liquid solvent. Second, the catalytic

* Corresponding author. Tel.: +1 201 216 5332; fax: +1 201 216 8306.
E-mail address: yvoloshi@stevens.edu (Y. Voloshin).

0920-5861/$ – see front matter © 2007 Elsevier B.V. All rights reserved.
doi:10.1016/j.cattod.2007.01.043

Nomenclature

a_{gl}	gas–liquid interfacial area per unit volume of reactor (m^2/m^3)
C_A	concentration of species A in liquid (mol/cm^3)
$C_{A,sat}$	saturated concentration of species A in liquid (mol/cm^3)
$D_{eff,A}$	overall effective molecular diffusivity of species A in the gas–liquid mixture ($=D_A = D_{A,G}x_G + D_{A,L}x_L$) ($cm^2/s$)
$D_{eff,A,G}$	effective molecular diffusivity of species A in the gas phase (cm^2/s)
$D_{eff,A,L}$	effective molecular diffusivity of species A in the liquid phase (cm^2/s)
E_a	activation energy (kJ/mol)
F	volumetric flow rate of reactants or products (m^3/s)
ΔH	enthalpy of reaction (kJ/mol)
P_A	partial pressure of species A in the gas phase (psia)
r_a	intrinsic reaction rate with respect to species a (g/g cat/h)
R	ideal gas constant (kJ/mol K)
R_A	observed reaction rate with respect to species A (g/g Pd/h)
R_p	average radius of catalyst particles (m)
T_w	reactor wall temperature (K)
W	catalyst mass (g)
x_G	volumetric gas fraction
x_L	volumetric liquid fraction

Greek letters

λ_e	effective thermal conductivity of porous catalyst (W/m K)
ρ_p	density of catalyst particles (g/m^3)

reaction of hydrogen and oxygen involves several reaction pathways, most of which result in the production of water. A catalyst that maximizes the selectivity for H_2O_2 is critical for the viability of this process.

Major disadvantages of either the AO process or of the patented DC methods can be overcome by producing hydrogen peroxide in a microreactor. The DC reaction can be carried out safely with a high hydrogen concentration (in the regime that would be explosive in a large-scale reactor) because the width of microreactor channels is smaller than the quenching distance of hydrogen and oxygen radicals. In other words, much higher temperatures and pressures are required to start an explosion in a microchannel than in a macrochannel [15,16]. This makes the DC reaction intrinsically safe in a microreactor for all H_2/O_2 ratios and all process conditions that might be used for H_2O_2 production. The ability to use safely high hydrogen concentrations makes it unnecessary to use very high pressures to achieve significant reaction rates, thus avoiding the need for expensive high-pressure equipment. The DC process is not restrained by the requirements of high quantity and high concentration of the present AO process. Also, the distillation step of the AO process is eliminated, which leads to significant energy savings. Portability of the microreactors opens the possibility of installing microreactor plants at the end-users' sites, leading to greatly decreased transportation costs.

In this study, we describe the production of H_2O_2 in a microreactor by the direct combination process. Optimum operating conditions were found that enable us to obtain 1.3 wt% H_2O_2 using a catalyst prepared in-house. The H_2O_2 synthesis step was studied in a differential microreactor with the suppression of other reactions and kinetics of this reaction were obtained.

1.2. Reaction pathways involved in the DC process

Reactions that take place in parallel and in series in the synthesis of H_2O_2 by the DC process are shown in Scheme 1. H_2O_2 synthesis, the desired reaction, is numbered as reaction (1). Reaction (2) is direct formation of water, which is in parallel with reaction (1). Reaction (3) is decomposition of H_2O_2 by reduction, and reaction (4) is H_2O_2 decomposition by disproportionation. Both reaction (3) and reaction (4) are in series with reaction (1).

The main products of DC process are hydrogen peroxide and water. The optimum catalyst and operating conditions are such that will improve the yield of H_2O_2 by favoring reaction (1), while suppressing reactions (2)–(4) as much as possible.

A growing number of researchers who studied the DC process focused on determining the reaction mechanisms, and on clarifying the relative importance of the multiple reactions. The earliest work on direct formation of H_2O_2 in scientific literature was done by the group of Pospelova [18–20], who described the essential properties of this system and proposed a mechanism for H_2O_2 synthesis that involved dissociative adsorption of H_2 on an active site consisting of two palladium atoms, non-dissociative adsorption of O_2 on the same site, and a surface reaction between H_2 and O_2 to form H_2O_2 through a HO_2^- intermediate. The same group also found that certain halide salts and acids can act as promoters for H_2O_2 formation. The fact that O–O bond does not dissociate during H_2O_2 formation was experimentally confirmed by Dissanyake and Lunsford [21] and the presence of HO_2^- on catalyst surface during the reaction was discovered by Sivadinarayana et al. [22].

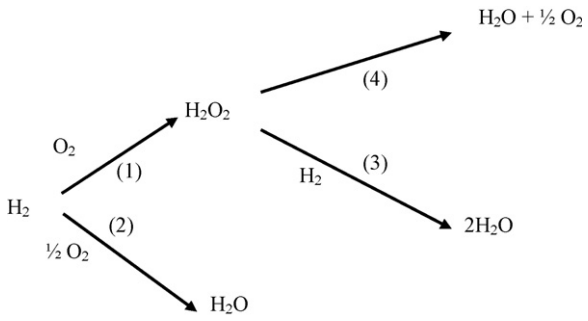

Scheme 1. Reactions involved in the formation of hydrogen peroxide [17].

The promoting effect of halides on formation of H_2O_2 was clarified by Chinta and Lunsford [23], who demonstrated that Br^- inhibits the direct formation of water, rather than slows down either the reduction or decomposition of H_2O_2, most likely by poisoning the catalytic sites active in breaking the O–O bond to form water [24]. Cl^- has the same effect as Br^-, but higher concentrations are required [25]. When H^+ is present in sufficient concentration in the reaction medium, reaction (3) is suppressed and can be neglected, so that H_2O_2 is consumed only through reaction (4) [17,23].

The sole attempt to determine the kinetics of DC reactions was made by Melada et al. [26], who obtained power law rate constants for reactions (1)–(3) by non-linear regression of a system of simultaneous equations with mass balances of all components. The experiments were run with gas compositions below the explosive limit and the disproportionation reaction (4) was found to be negligible at their experimental conditions. However, these rate expressions cannot be used to predict the rate of direct H_2O_2 formation at higher hydrogen concentrations (above the explosive limit) because catalytic reactions can be approximated by a power law only at a low coverage of the catalyst surface [27]. A rate expression that takes into account the effect of surface coverage on the reaction rate, such as a Langmuir–Hinshelwood expression, is more appropriate for a complete description of the kinetics.

The goal of this work is to obtain Langmuir–Hinshelwood rate expressions that can be used for rational design of a microreactor for production of hydrogen peroxide. A complete and usable rate expression at high H_2 concentrations has not been obtained in the past because of the danger and complexity of this reaction. In this work, instead of regressing the complete mass balance for Eqs. (1)–(4), we decided to obtain the kinetics of each reaction separately by isolating them. Operating conditions were found where reactions (1) and (3) could be isolated and studied one at a time, while reactions (2) and (4) were negligible. The conditions were as follows:

1.2.1. Synthesis (reaction (1))

We found that the selectivity of this reaction for H_2O_2 is 100% when the conversion of reactants is very small (less than approximately 2% for H_2).

1.2.2. Direct formation of water (reaction (2))

This reaction can be neglected when the selectivity for H_2O_2 is 100%.

1.2.3. Reduction (reaction (3))

This reaction was isolated by using a mixture of hydrogen and nitrogen in the gas phase and an H_2O_2 solution with 1% (w/w) H_2SO_4 and 10 ppm NaBr in the liquid phase.

1.2.4. Disproportionation (reaction (4))

This reaction was found to be negligible when 1% (w/w) H_2SO_4 and 10 ppm NaBr were present in the solvent.

Thus, when the rate expressions for reactions (1) and (3) are known, the overall kinetics of H_2O_2 formation can be expressed as

$$r_{H_2O_2} = r_1 - r_3. \quad (1)$$

2. Experimental methods

2.1. Materials

The reactants for H_2O_2 synthesis were hydrogen (Ultra High Purity, Praxair) and oxygen in the form of air (Extra Dry, Praxair), which were passed through a 2-μm filter before entering the reactor. Nitrogen (Ultra High Purity, Praxair) was used to dilute the gas stream. The liquid phase consisted of deionized water with 1% (w/w) H_2SO_4 (A.C.S. reagent grade, 95–98%, Aldrich), and 10 ppm NaBr (Aldrich) as promoters and stabilizers of H_2O_2.

2.2. Catalyst preparation

The catalyst used for all experiments was 2% Pd on SiO_2, prepared by the sol–gel method with $PdCl_2$ as the source of palladium. The gel was prepared from tetraethoxysilane (TEOS), ethanol and water [28] and calcined. The calcined catalyst was ground and sieved to obtain particles with a diameter between 75 and 150 μm. Surface area of the catalyst was 603 m^2/g (multi-point BET technique, using Quantochrome Instruments Autosorb-1) and a dispersion of 18.1% (FEG-TEM, Model CM20, Philips, Eindhoven, Netherlands). A total of six batches of catalyst were prepared using this procedure, each batch producing H_2O_2 at a space–time yield within 5% of the average STY when tested at identical conditions, thus demonstrating the reproducibility of the catalyst.

2.3. H_2O_2 synthesis

A schematic of the experimental set-up used for all experiments is shown in Fig. 1. The flow rates of hydrogen, oxygen (as air) and nitrogen were controlled by mass flow controllers (Porter Model 201). Flow rate of the solvent was controlled by an HPLC pump (Lab Alliance Series III) and the solvent was combined with mixed gas in a PTFE micromixer (Upchurch). All streams flowed in (1/16) in. 316L SS tubing with 765 μm i.d. The microreactor consisted of the same type of tubing packed with catalyst, enclosed with filters of polypropylene wool for retaining the catalyst, and connected to the system horizontally with PTFE fittings (Upchurch). Amount of the catalyst packed into the microreactor varied between 4 and 21 mg. Length of the microreactor was chosen such that about 2–3 cm of empty tubing would remain after the catalyst was packed. The empty space was then packed with glass beads of the same size range as the catalyst in order to prevent the catalyst particles from blocking the retaining filter at the downstream end of the reactor.

As safety precautions, flame arrestors were installed on all gas lines downstream of the mass flow controllers and the gas

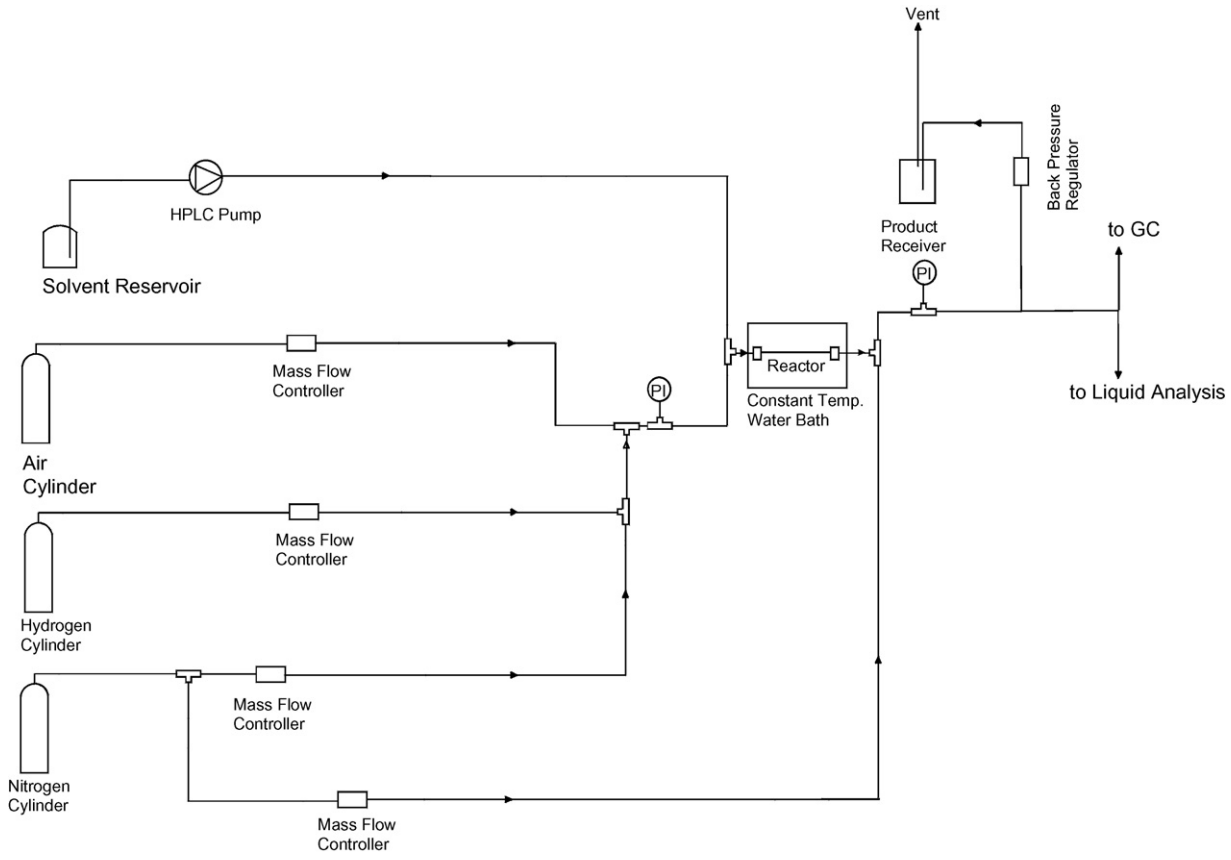

Fig. 1. Experimental set-up for synthesis of H_2O_2.

stream was diluted with nitrogen to a composition below the explosive limit prior to leaving (1/16) in. tubing at the system's outlet.

Temperature in the microreactor was controlled by immersing it in a constant-temperature water bath (Thermo-Haake DC10). Pressure was controlled by a back-pressure regulator (Circle Valve Technologies) and continuously recorded using LabView software. Concentration of H_2O_2 in the liquid phase was determined by titration with potassium permanganate and composition of the gas phase was measured by a Shimadzu GC-14B gas chromatograph with a Mole Sieve 5A column at 35 °C and argon as carrier gas. Pressure drop across the reactor varied between approximately 3 and 17% of the inlet pressure (depending on the total flow rate), however the average of pressures at the inlet and outlet of the reactor was maintained at 300 psig for all experiments, unless stated otherwise. The gas–liquid ratio was held constant at 440 (v/v, at standard conditions).

Productivity was expressed as space–time yield, calculated as

$$\mathrm{STY} = \frac{c_{\mathrm{H_2O_2}} F_{\mathrm{liq}}}{W}. \quad (2)$$

Conversion was calculated on the basis of the limiting reactant (H_2 or O_2) and selectivity was calculated using the following equation:

$$\text{selectivity} = \frac{\text{moles of } H_2O_2 \text{ formed}}{\text{moles of limiting reactant reacted}} \times 100\%. \quad (3)$$

The kinetic experiments were done in a differential reactor with 4 mg of catalyst, where length of the reactor was 4 cm, approximately 2 cm of which was packed with catalyst and the remainder with glass beads. Conversion of the limiting reactant was between 1 and 2%. At such small conversions, space–time yield can be assumed to be the intrinsic reaction rate. For all experiments, the reported reaction rates are steady state values measured after the reactor performance has been stabilized for about 2 h.

3. Results and discussion

3.1. Flow regime

Prior to determining the intrinsic kinetics of this reaction, conditions have to be found where the gradient of reactant concentrations between the bulk liquid and the catalyst surface is negligible. Calculation of the mass transfer rate requires the knowledge of the flow regime in the reactor because all known correlations of mass transfer coefficients apply at specific flow regimes. Flow regime in the microreactor at reaction conditions was determined by flow visualization experiments, which were

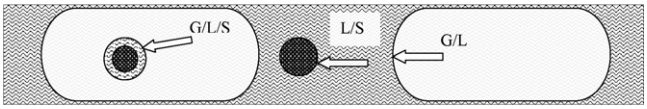

Fig. 2. Schematic of mass transfer steps in the microreactor. G/L: gas–liquid; L/S: liquid–solid; G/L/S: gas–solid through a thin liquid film.

carried out by replacing the reactor with a transparent glass tube with a square cross-section measuring 500 μm × 500 μm. The flow regime commonly seen in empty channels and at the flow rates and channel dimensions used in this work is known as Taylor flow [29]. This was confirmed for our system. When the tube was packed with glass beads of the same size range as the catalyst, the flow was still separated into distinct gas and liquid slugs, but it was no longer typical Taylor flow because of the continuous breaking of liquid slug boundaries by the glass beads and long mist-like tails trailing behind liquid slugs. Fig. 2 shows a simplified schematic of the mass transfer steps in the microreactor, where the flow regime is approximated by Taylor flow. The mass transfer takes place by diffusion and can be separated into three steps: from gas to liquid, from liquid directly to solid, and from gas to solid through a thin liquid film.

3.2. External mass transfer gradient

A commonly used criterion for determining the relative importance of an external mass transfer gradient is given by Mills and Chaudhari [30]:

$$\frac{R_A}{k_{gl}a_{gl}C_{A,sat}} < 0.1. \tag{4}$$

For the system used here, the mass transfer coefficient cannot be directly calculated because all of the known correlations of mass transfer coefficients, such as the ones for trickle or bubble flow in a packed bed [31] or Taylor flow in an empty tube [32], cannot be applied to Taylor flow in a packed bed. Instead, the presence of an external mass transfer limitation was determined experimetally by varying the flow velocity while keeping the residence time, or the F/W ratio, constant. Velocity affects the gas–liquid mass transfer by

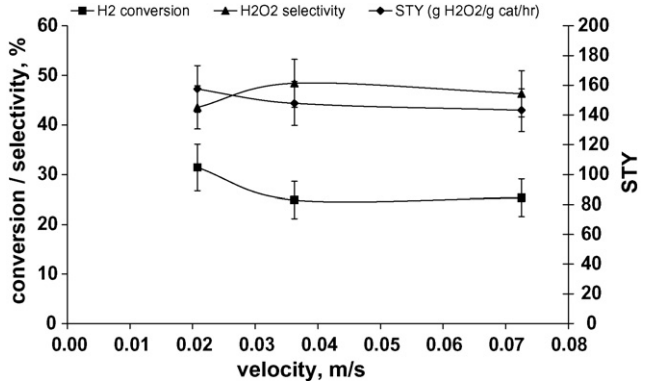

Fig. 3. Effect of total flow velocity on formation of H_2O_2. *Reaction conditions*—gas composition: 9.1% H_2 in air, total pressure = 300 psig, T = 50 °C, residence time (in empty reactor) = 1.1 s.

increasing the circulation inside liquid slugs and by decreasing the thickness of liquid film covering the catalyst particles. The results (Fig. 3) show that the reaction rate does not depend on flow velocity, which implies that the reactant concentration gradient between the catalyst surface and the bulk liquid phase is insignificant compared to the bulk liquid concentrations as long as the total superficial flow velocity is above 0.02 m/s. Thus, we can consider the criterion in Eq. (4) satisfied, which allows us to calculate the minimum mass transfer coefficient by setting the ratio in Eq. (4) equal to unity. This results in a lower limit for $k_{gl}a_{gl}$ of 8 s^{-1} (calculated at 150 g H_2O_2/g Pd/h), which is in the range of $k_{gl}a_{gl}$ values obtained by Losey at al. [33] in a packed-bed microreactor (5–15 s^{-1}).

3.3. Internal mass transfer and heat transfer gradients

Ratio of the observed reaction rate to the internal diffusion rate in the porous catalyst is given by the Weisz modulus:

$$M_W = \frac{R_{H_2}\rho_p {R_p}^2}{D_{eff,H_2}C_{H_2,sat}}. \tag{5}$$

Pore diffusion limitations can be considered absent when $M_w \ll 1$. Effective diffusivities, calculated using the typical range of values of porosity (0.4–0.6), tortuosity (2–8) and constriction factor (0.7–0.8) [34], were estimated for the gas and liquid phases, and then used to calculate the overall effective diffusivity by scaling the values for each phase by the fractions of that phase in the reactor feed. At the highest reaction rate measured in kinetic experiments (316 g H_2O_2/g Pd/h), the Weisz modulus was calculated to be between 0.09 and 0.25, implying negligible pore diffusion limitations.

Mears [35] derived a criterion for determining the presence of an interparticle heat transfer limitation. If the inequality in Eq. (6) is satisfied, then the radial temperature difference in the reactor is no more than 5%:

$$\frac{|-\Delta H(-r_{H_2}){d_p}^2|}{\lambda_e T_w} < 0.4\frac{RT_w}{E_a}. \tag{6}$$

Effective thermal conductivity, λ_e, was estimated to be 0.1 W/m K, which is a typical value for porous catalysts [36]. The left-hand side of Eq. (6) is calculated to be seven orders of magnitude smaller than the right-hand side, so that we can consider the microreactor to be isothermal.

3.4. Effects of temperature and pressure

Experiments were carried out at various pressures and temperatures in order to find the optimum parameters for production of 1 wt% H_2O_2 and for further kinetic experiments. Effect of temperature on the reactor performance can be seen in Fig. 4. Space–time yield, conversion and selectivity increase with temperature and then stabilize. The initial increase in selectivity must be due to the rate of synthesis reaction increasing with temperature faster than the rate of reduction, which implies that the activation energy of synthesis is higher

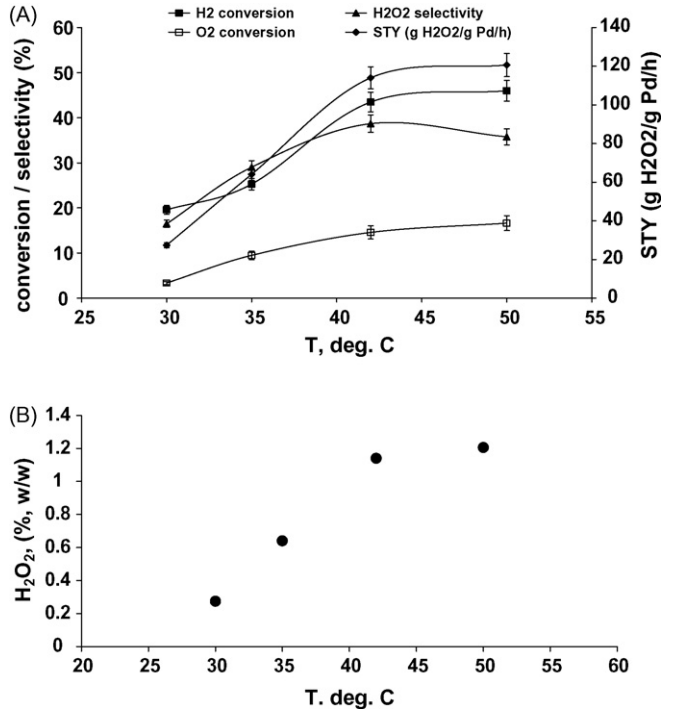

Fig. 4. Effect of temperature on formation of H_2O_2: (A) H_2 conversion, H_2O_2 selectivity, and space–time yield; (B) concentration of H_2O_2 at reactor's outlet. *Reaction conditions*—gas composition: 9.1% H_2 in air, total pressure = 300 psig, gas flow rate = 22 ml/min (at standard temperature and pressure), liquid flow rate = 0.05 ml/min, 15 mg of catalyst.

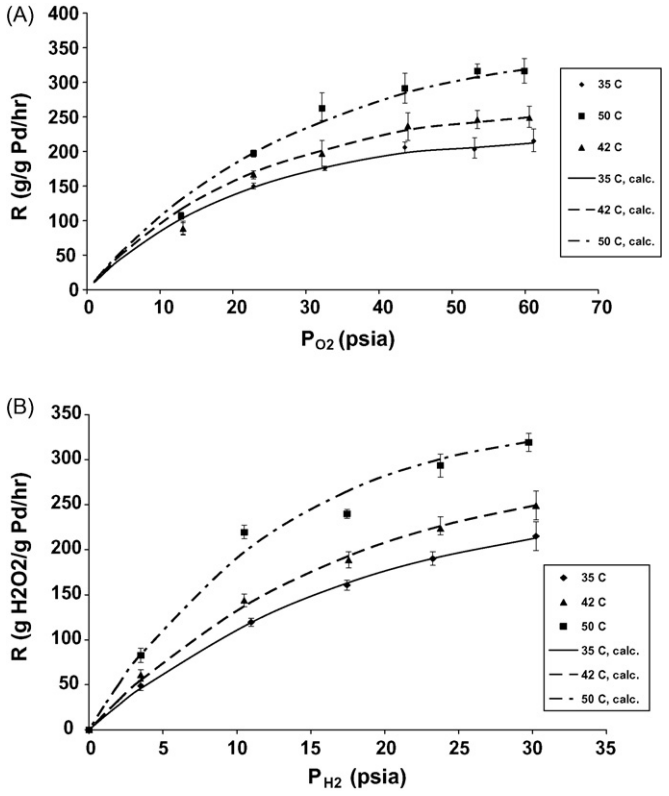

Fig. 6. Kinetic data and reaction rates predicted by mechanism 4. (A) P_{H_2} = 30 psig, total pressure = 300 psig. (B) P_{O_2} = 63 psig, total pressure = 300 psig.

than that of reduction. All three curves become independent of temperature above 42 °C.

Fig. 5 shows the effect of total pressure. The residence time was kept constant by maintaining a constant F/W ratio. Selectivity increases, while H_2 and O_2 conversions decrease with pressure, and then stabilize above 200 psia, while the space–time yield increases almost linearly with pressure. The increase in selectivity with pressure may be due to one of, or both, of two factors: (1) the rate of reaction (1) may have a stronger dependence on the partial pressures of hydrogen and oxygen than the rate of reaction (3), and (2) the direct formation of water may be significant at lower pressures, but decreases at 300 psig. The decrease in O_2 conversion, and the fact that selectivity for H_2O_2 is 100% at 300 psig and with very small conversions (<2%), support the second explanation. Based on the data in Figs. 4 and 5, kinetic experiments were carried out at an average total pressure of 300 psig and at 35–50 °C because the selectivity and productivity are highest at these conditions.

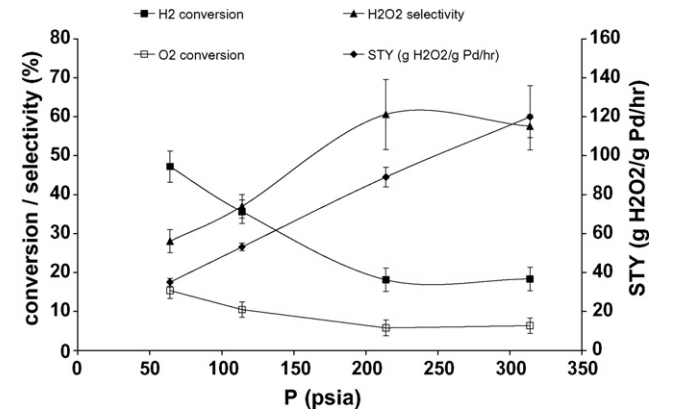

Fig. 5. Effect of total pressure on formation of H_2O_2. *Reaction conditions*—gas composition: 9.1% H_2 in air, T = 42 °C, residence time (in empty reactor) = 1.1 s.

3.5. Kinetic experiments

Kinetic data for the synthesis of H_2O_2 is shown in Fig. 6. The data in Fig. 6A were obtained by varying P_{O_2} while keeping the total pressure and P_{H_2} constant by corresponding adjustments in flow rates of N_2 and air. Similarly, in Fig. 6B, P_{O_2} and the total pressure were kept constant and P_{H_2} varied. We propose three possible mechanisms for the synthesis reaction (mechanisms 1–3 in Table 1), such that each mechanism follows the general reaction scheme described by Pospelova et al. [18], as mentioned above. A fourth mechanism was proposed by Zhou and Lee [14], named mechanism 4 in Table 1. Langmuir–Hinshelwood rate expressions were derived based on each of the mechanisms and are also shown in Table 1. Surface reaction was assumed to be the rate-determining step for all four mechanisms because the reaction rate becomes independent of reactant concentrations as the concentrations increase and then slowly decreases, which implies that the adsorption steps are in equilibrium. Mechanism 4 was selected as the best-fitting

Table 1
Proposed mechanisms for synthesis of H_2O_2 (*catalytic site)

Mechanism no.	Mechanism	Rate law
1	$H_2 + 2^* \rightarrow 2H^*$ $H^* + O_2 \rightarrow {}^*HO_2$ $H^* + {}^*HO_2 \rightarrow H_2O_2 + 2^*$	$r = \frac{k_3 K_{H_2} K_{O_2} P_{H_2} P_{O_2}}{\left(1+(K_{H_2}P_{H_2})^{1/2}+K_{O_2}(K_{H_1}P_{H_2})^{1/2}P_{O_2}\right)^2}$
2	$H_2 + {}^{**} \rightarrow H^{**}H$ $^* + O_2 \rightarrow {}^*O_2$ ${}^*O_2 + H^{**}H \rightarrow H^{**}HO_2 + {}^*$ $H^{**}HO_2 \rightarrow H_2O_2 + {}^{**}$	$r = \frac{k_3 K_{H_2} K_{O_2} P_{H_2} P_{O_2}}{\left(1+(K_{H_2}P_{H_2})^{1/2}+K_{O_2}P_{O_2}\right)^3}$
3	$H_2 + {}^{**} \rightarrow H^{**}H$ $^{**} + O_2 \rightarrow {}^{**}O_2$ ${}^{**}O_2 + H^{**}H \rightarrow H^{**}HO_2 + {}^{**}$ $H^{**}HO_2 \rightarrow H_2O_2 + {}^{**}$	$r = k_3 K_{H_2} K_{O_2} P_{H_2} P_{O_2} \left(\frac{1+(1+2K_{H_2}P_{H_2}2K_{O_2}P_{O_2})^{1/2}}{K_{H_2}P_{H_2}+K_{O_2}P_{O_2}}\right)^4$
4	$H_2 + {}^* \rightarrow {}^*H_2$ $O_2 + {}^* \rightarrow {}^*O_2$ ${}^*O_2 + {}^*H_2 \rightarrow H^{**}HO_2$ $H^{**}HO_2 \rightarrow H_2O_2 + {}^{**}$	$r = \frac{k_3 K_{H_2} K_{O_2} P_{H_2} P_{O_2}}{\left(1+K_{H_2}P_{H_2}+K_{O_2}P_{O_2}\right)^2}$

Table 2
Kinetic constants of reaction (1) at different temperatures

T (°C)	R^2	k (g H_2O_2/g Pd/h)	K_{H_2} (psi^{-1})	K_{O_2} (psi^{-1})
35	0.99958	1619.24 ± 141.17	0.0386 ± 0.0061	0.027 ± 0.0035
42	0.99863	1897.68 ± 317.10	0.0391 ± 0.012	0.025 ± 0.0065
50	0.98668	2424.86 ± 232.97	0.046 ± 0.0094	0.021 ± 0.0040

Table 3
Arrhenius constants of reaction (1)

	k	K_{H_2}	K_{O_2}
Activation or adsorption energy (kJ/mol)	22.34	10.05	−12.19
Pre-exponential factor	9.81×10^{-6} g H_2O_2/g Pd/hr	1.90 psi^{-1}	2.33×10^{-4} psi^{-1}

model because it had the highest R^2 values of kinetic and Arrhenius curves. Values of the kinetic parameters with their 95% confidence intervals (Table 2) were calculated by non-linear regression using the Levenberg–Marquardt algorithm. Comparison of the kinetic data with the values predicted by mechanism 4 is shown in Fig. 6 (where the error bars are based on at least two replications). Conversion and selectivity were measured only for the points with highest concentrations of reactants because it was confirmed that, if the selectivity is 100% at higher concentrations of the reactants, then it will remain at 100% when the concentration of reactants, and consequently the reaction rates, are decreased, as long as the total flow rates and catalyst amount (i.e. residence time) were kept constant.

Table 3 shows the calculated Arrhenius constants of the kinetic parameters. The activation energy (22.34 kJ/mol) can be compared to that of a similar reaction with the same number of bonds broken and formed, namely the hydrogenation of ethylene. Experimental measurements of the activation energy for this reaction range between 25.1 and 46 kJ/mol [37], which is close to the activation energy of H_2O_2 synthesis determined here.

4. Conclusion

A packed-bed microreactor for direct production of hydrogen peroxide at moderate temperature and pressure was demonstrated. The reactor was operated at varied temperatures and pressures in order to find optimum conditions for the production of 1 wt% H_2O_2. Effect of flow velocity at a constant F/W ratio was negligible, which implies that the reaction is kinetically controlled, as opposed to mass transfer controlled. Internal mass transfer and heat transfer limitations were found to be negligible. Since the direct combination process is actually a network of reactions involving synthesis and consumption of H_2O_2, the rate expressions for each reaction must be determined and then combined into an overall rate expression. In this paper, the rate expression for H_2O_2 synthesis was obtained by operating the microreactor at 100% selectivity for H_2O_2, thus isolating the synthesis reaction.

It is a common practice to verify rate expressions obtained using a differential reactor by comparing experimental and predicted reaction rates in an integral reactor. In case of reaction (1), such verification is impossible because the selectivity for H_2O_2 decreases below 100% at conversions higher than those in

a differential reactor. The rate expressions described in this study will be verified and reported in a future publication, where the determination of kinetics of reaction (3) will be described and Eq. (1) will be used to predict the rates of H_2O_2 formation in an integral reactor.

Acknowledgements

The authors would like to thank the U.S. Department of Energy (Office of Industrial Technologies) for financial support under contract DE-FC36-02ID14427, and FMC Corporation for their technical contribution to the program. Y. Voloshin would also like to thank the Robert C. Stanley Graduate Fellowship Program. In addition, we are grateful to the individuals who provided valuable help to this project: Ms. Sunitha Tadepalli, Dr. James Manganaro, Dr. Emmanuel Dada, Dr. Dalbir Sethi, Dr. Lucie Bednarova, Dr. Haibiao Chen, Dr. Dongying Qian, and Prof. Suphan Kovenklioglu.

References

[1] Kirk-Othmer, Encyclopedia of Chemical Technology, 5th ed., John Wiley and Sons, 2004.
[2] Ullman's, Encyclopedia of Industrial Chemistry, 7th ed., John Wiley and Sons, 2005.
[3] H.N. Quan, A.L. Teel, R.J. Watts, Effect of contaminant hydrophobicity on hydrogen peroxide dosage requirements in the Fenton-like treatment of soils, J. Hazard. Mater. 102 (2003) 277–289.
[4] H. Henkel, W. Weber, Manufacture of hydrogen peroxide, U.S. Patent 1,108,752 (1914).
[5] G.W. Hooper, Catalytic production of hydrogen peroxide from its elements, U.S. Patent 3,336,112 (1967).
[6] Y.H. Izumi, S. Miyazaki, Kawahara, Process for preparing hydrogen peroxide, U.S. Patent 4,009,252 (1977).
[7] A.I. Dalton, R.W. Skinner, Synthesis of hydrogen peroxide, U.S. Patent 4,336,239 (1982).
[8] M. Kawakami, Y. Ishiuchi, H. Nagashima, T. Tomita, Y. Hiramatsu, Process for producing hydrogen peroxide, U.S. Patent 5,399,334 (1995).
[9] L.W. Gosser, Catalytic process for making H_2O_2 from hydrogen and oxygen, U.S. Patent 4,681,751 (1988).
[10] M. Fischer, T. Butz, K. Masonne, Preparation of hydrogen peroxide from hydrogen and oxygen, U.S. Patent 6,872,377 (2005).
[11] M. Paoli, Process for the production of hydrogen peroxide from hydrogen and oxygen, U.S. Patent 5,194,242 (1993).
[12] A. Germain, J. Pirard, V. Delattre, J. Van Weynbergh, C. Vogels, Process for the manufacturing of hydrogen peroxide by direct synthesis from hydrogen and oxygen, U.S. Patent 5,500,202 (1996).
[13] K.T. Chuang, B. Zhou, Production of hydrogen peroxide, U.S. Patent 5,338,531 (1994).
[14] B. Zhou, L. Lee, Supported noble metal, phase controlled catalyst and methods for making and using the catalyst, U.S. Patent 6,919,065 B2 (2005).
[15] M.T. Janicke, H. Kestenbaum, U. Hagendorf, F. Schuth, M. Fichtner, K. Schubert, The controlled oxidation of hydrogen from an explosive mixture of gases using a microstructured reactor/heat exchanger and Pt/Al_2O_3 catalyst, J. Catal. 191 (2000) 282–293.
[16] G. Veser, Experimental and theoretical investigation of H_2 oxidation in a high-temperature catalytic microreactor, Chem. Eng. Sci. 56 (2001) 1265–1273.
[17] P. Landon, P.J. Collier, A.F. Carley, D. Chadwick, A.J. Papworth, A. Burrows, C.J. Kiely, G.J. Hutchings, Direct synthesis of H_2O_2 from H_2 and O_2, Phys. Chem. Chem. Phys. 5 (2003) 1917–1923.
[18] T.A. Pospelova, N.I. Kobozev, E.N. Eremin, Palladium catalyzed synthesis of hydrogen peroxide form its elements. I. Conditions for the formation of hydrogen peroxide, Russ. J. Phys. Chem. 35 (1961) 143–147.
[19] T.A. Pospelova, N.I. Kobozev, Palladium catalyzed synthesis of hydrogen peroxide form its elements. II. Active centres of palladium, Russ. J. Phys. Chem. 35 (1961) 262–265.
[20] T.A. Pospelova, N.I. Kobozev, Palladium catalyzed synthesis of hydrogen peroxide form its elements. III. Active centres for the catalytic decomposition of hydrogen peroxide on palladium, Russ. J. Phys. Chem. 35 (1961) 584–587.
[21] D.P. Dissanyake, J.H. Lunsford, The direct formation of H_2O_2 from H_2 and O_2 over colloidal palladium, J. Catal. 214 (2003) 113–120.
[22] C. Sivadinarayana, T.V. Choudhary, L.L. Daemen, J. Eckert, D.W. Goodman, The nature of the surface species formed on Au/TiO_2 during the reaction of H_2 and O_2: an inelastic neutron scattering study, J. Am. Chem. Soc. 126 (2004) 38–39.
[23] S. Chinta, J.H. Lunsford, A mechanistic study of H_2O_2 and H_2O formation rom H_2 and O_2 catalyzed by palladium in an aqueous medium, J. Catal. 225 (2004) 249–255.
[24] R. Burch, P.R. Ellis, An investigation of alternative catalystic approaches for the direct synthesis of hydrogen peroxide from hydrogen and oxygen, Appl. Catal. B: Environ. 42 (2003) 203–211.
[25] Q. Liu, J.H. Lunsford, The roles of chloride ions in the direct formation of H_2O_2 from H_2 and O_2 over a Pd/SiO_2 catalyst in a H_2SO_4/ethanol system, J. Catal. 239 (2006) 237–243.
[26] S. Melada, R. Rioda, F. Menegazzo, F. Pinna, G. Strukul, Direct synthesis of hydrogen peroxide on zirconia-supported catalysts under mild conditions, J. Catal. 239 (2006) 422–430.
[27] A. Vannice, Kinetics of Catalytic Reactions, Springer Science, 2005.
[28] P.A. Robles-Dutenhefner, D.L. Nunes, J.A. Goncalves, E.V. Gusevskaya, E.M.B. Sousa, Sol–gel palladium composites: effect of thermal treatment on the catalytic activity, J. Non-Cryst. Solids 348 (2004) 195–200.
[29] M.T. Kreutzer, F. Kapteijn, J.A. Moulijn, J.J. Heiszwolf, Multiphase monolith reactors: chemical reaction engineering of segmented flow in microchannels, Chem. Eng. Sci. 60 (2005) 5895–5916.
[30] P.L. Mills, R.V. Chaudhari, Multiphase catalytic reactor engineering and design for pharmaceuticals and fine chemicals, Catal. Today 37 (1997) 367–404.
[31] C.N. Satterfield, Mass Transfer in Heterogeneous Catalysts, MIT Press, 1970 (chapter 2).
[32] G. Bercic, A. Pintar, The role of gas bubbles and liquid slug lengths on mass transport in Taylor flow through capillaries, Chem. Eng. Sci. 52 (1997) 3709–3719.
[33] M.W. Losey, M.A. Schmidt, K.F. Jensen, Microfabricated multiphase packed-bed reactors: characterization of mass transfer and reactions, Ind. Eng. Chem. Res. 40 (2001) 2555–2562.
[34] H.S. Fogler, Elements of Chemical Reaction Engineering, Prentice-Hall, Englewood Cliffs, NJ, 1992 (chapter 12).
[35] D.E. Mears, Diagnostic criteria for heat transfer limitations in fixed bed reactors, J. Catal. 20 (1971) 127–131.
[36] C.S. Sharma, P. Harriott, R. Hughes, Thermal conductivity of catalyst pellets and other porous particles. Part II. Experimental measurements, Chem. Eng. J. 10 (1975) 73–80.
[37] E.W. Hansen, M. Neurock, First-principles-based Monte Carlo simulation of ethylene hydrogenation kinetics on Pd, J. Catal. 196 (2000) 241–252.